Modification of local electronic state by BEDT-STF doping to κ-(BEDT-TTF)$_2$Cu[N(CN)$_2$]Br salt studied by ^{13}C NMR spectroscopy

T. Kobayashi, Y. Ihara,* and A. Kawamoto

Department of Condensed Matter Physics, Graduate School of Science, Hokkaido University, Sapporo 060-0810, Japan

(Received 28 September 2015; revised manuscript received 16 February 2016; published 14 March 2016)

We present the results of site-selective ^{13}C NMR spectroscopy on an organic superconductor κ-(BEDT-TTF)$_2$Cu[N(CN)$_2$]Br (κ-Br) doped with BEDT-STF molecules. We reveal microscopically the modulation of the local electronic state caused by the BEDT-STF doping from the ^{13}C NMR measurement on two types of samples, which are ^{13}C enriched κ-Br doped with naturally abundant BEDT-STF molecules, and natural κ-Br doped with ^{13}C enriched BEDT-STF molecules. The results of the nuclear spin-lattice relaxation rate $1/T_1$ measured both in the normal and superconducting state suggest that the potential disorder at the BEDT-STF sites scatters antiferromagnetic interaction and superconducting Cooper pairs.

DOI: 10.1103/PhysRevB.93.094515

I. INTRODUCTION

The superconducting (SC) pair breaking effect brought about by impurities has been studied intensively to identify the SC properties of pure materials [1]. For superconductors with an isotropic SC gap, the SC transition temperature T_c can be suppressed to zero by doping only a few percent of the magnetic impurities, while T_c is not susceptible to the nonmagnetic impurities [2]. In contrast, anisotropic superconductors are more susceptible to nonmagnetic impurities than magnetic ones [3]. This qualitatively different behavior can be used to identify the symmetry of a SC gap. However, the microscopic mechanisms for how the different impurities scatter the SC pairs have not yet been revealed experimentally. As the electronic state becomes inhomogeneous in doped materials, we should study the local electronic state near the impurity site using a microscopic probe to understand the SC pair breaking mechanism brought about by impurity scattering. Sophisticated NMR experiment in a cuprate superconductor $YBa_2Cu_3O_{6+x}$ (YBCO) revealed that nonmagnetic Zn doping induces staggered moments near the impurity sites [4]. NMR spectroscopy is thus a powerful technique to study inhomogeneous electronic states with impurities.

The impurity doping effects have not been studied in organic superconductors because the electrochemical oxidation process excludes impurities from the obtained single crystals. For the impurities to enter into the crystal, we need to prepare molecules that have nearly the same molecular structure as the molecules in the pure crystal. In the case of BEDT-TTF [bis(ethylenedithio)tetrathiafulvalene] -based organic salts, as the BEDT-TTF molecules were found to be replaced with the BEDT-STF [bis(ethylenedithio)diselenadithiafulvalene] molecules up to 25%, we can explore the BEDT-STF doping effects on organic superconductors [5]. Previous resistivity measurement on BEDT-STF-doped κ-(BEDT-TTF)$_2$Cu[N(CN)$_2$]Br (κ-Br) salt revealed that T_c decreases with BEDT-STF concentration. One possible interpretation is that the BEDT-STF molecules scatter SC pairs as an impurity. However, in addition to the suppression of T_c, the BEDT-STF doping induces a metallic resistivity in the normal state. Therefore, we cannot exclude the possibility that the chemical pressure effects from BEDT-STF doping modify the electronic band structure. To establish the BEDT-STF doping effects, the electronic properties in the doped sample should be investigated.

In this study, we doped BEDT-STF molecules into κ-Br salt and performed ^{13}C NMR spectroscopy. The ^{13}C NMR study on BEDT-STF-doped salts provides important information because we can observe selectively the electronic properties at the BEDT-TTF sites and the BEDT-STF sites by doping naturally abundant BEDT-STF molecules into ^{13}C enriched κ-Br salt (BEDT-TTF sites), and by doping the ^{13}C enriched BEDT-STF molecules into the naturally abundant κ-Br salt (BEDT-STF sites). From the results of four different samples including pristine κ-Br, we discuss the BEDT-STF doping effects on the normal state electronic properties and on the SC state.

II. EXPERIMENT

A. Sample preparation

In this study, we doped the BEDT-STF molecules, on which two sulfur atoms close to the central C=C bonds are replaced with selenium. We prepared four kinds of molecules: ^{13}C-enriched (hot) BEDT-TTF (A), naturally abundant (cold) BEDT-TTF (B), hot BEDT-STF (C), and cold BEDT-STF molecules (D) [Fig. 1(a)]. For the hot BEDT-TTF molecule, only one side of the central C=C bond is enriched with ^{13}C to eliminate the NMR spectral splitting due to nuclear spin-spin coupling [6], and for the hot BEDT-STF molecule the carbon nuclei at the sulfur side of the central C=C bond are selectively enriched. From these molecules, we prepared two types of κ-Br salts, TTF-x and STF-x, which are obtained by doping D to A and C to B, respectively. Here, x represents the BEDT-STF concentration of each sample. The BEDT-STF molecules can enter into the BEDT-TTF crystal by desolving both BEDT-STF and BEDT-TTF molecules during the electrochemical oxidation process [5]. The typical dimension of an obtained single crystal is $2.7\times2.5\times0.5$ mm^3. We confirmed via x-ray microprobe analysis that the BEDT-STF molecules enter into the crystal uniformly.

The SC diamagnetism of BEDT-STF-doped samples was observed by magnetization measurement (quantum design,

*yihara@sci.phys.hokudai.ac.jp

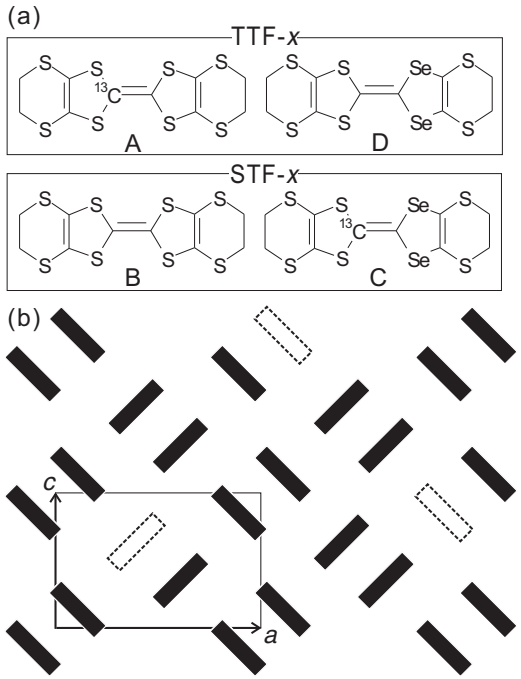

FIG. 1. (a) Four kinds of molecules prepared for this study. The NMR active ^{13}C isotope is selectively enriched in BEDT-TTF molecules in TTF-x, which is made of A and D, and in BEDT-STF molecules in STF-x, which is made of B and C. (b) A schematic in-plane structure of BEDT-STF doped κ-Br salt. Black and white molecules represent the BEDT-TTF and BEDT-STF, respectively.

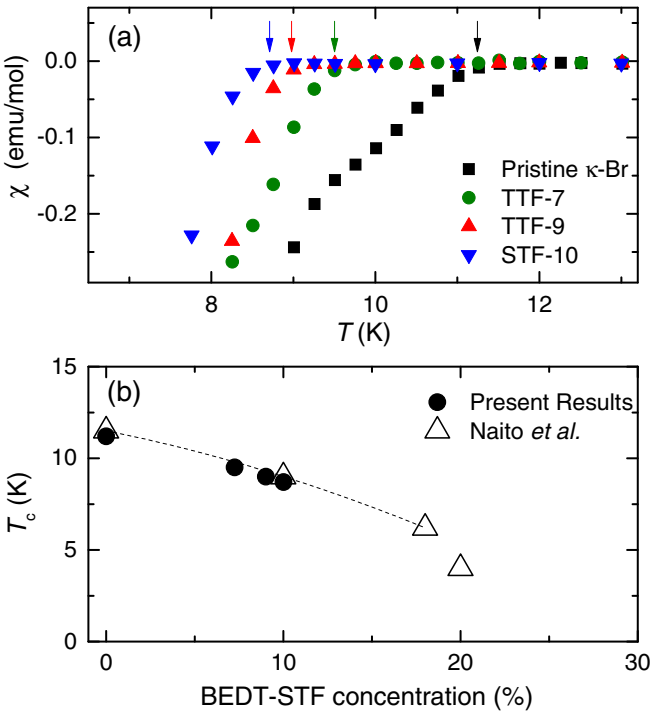

FIG. 2. (a) The onset of Meissner signals determined by the magnetization measurements. The arrows indicate the SC transition temperature T_c. A decrease in T_c was observed in the BEDT-STF doped samples, but the SC transition is as sharp as that in the pristine κ-Br. (b) The relationship between T_c and BEDT-STF concentration established by Naito *et al.* [5]. Closed circles represent T_c of our samples. The BEDT-STF concentrations of our samples were determined from this relation.

MPMS). As shown in Fig. 2(a), the SC transition of the doped sample is as sharp as that of the pristine sample, which indicates that the BEDT-STF molecules are doped uniformly into the crystal. We determined the actual BEDT-STF concentration x by comparing T_c of each sample with the previously established x to T_c relation [Fig. 2(b)] [5]. As shown in Table I, the determined x values (7%, 9%, and 10%) are smaller than the nominal values (8%, 15%, and 15%), because the solubility of BEDT-STF molecules is smaller than that of BEDT-TTF molecules.

B. Magnetization measurement

The temperature dependence of the uniform spin susceptibility χ_0 was measured for one single crystal of TTF-9 below 150 K. A magnetic field of 4 T was applied perpendicular to the conduction plane. The result is shown in Fig. 3 together with the susceptibility of the pristine sample, which was reported in the literature [7,8]. The data of the present study are more scattered than the reported data for the pristine sample, because we measured χ_0 of only one single crystal. In Fig. 3, the core diamagnetic contribution of -4.7×10^{-4} emu/mol is already subtracted. At temperatures higher than 100 K, TTF-9 shows identical behavior to the pristine sample. A difference between TTF-9 and the pristine sample is observed below 50 K. In the pristine sample, χ_0 starts to decrease below 50 K, and it shows a kink at 35 K as denoted by the upward arrow in Fig. 3. The temperature dependence becomes weak below 35 K. Around the corresponding temperatures, resistivity and NMR experiments revealed the suppression of antiferromagnetic (AF) fluctuations [7]. As χ_0 is suppressed by the increase in AF fluctuations, the change in slope at 35 K is also interpreted as an outcome of the decrease in AF fluctuations [9]. In TTF-9, χ_0 deviates from that for the pristine sample below 45 K. This result suggests that the BEDT-STF doping suppresses the AF fluctuations from a temperature higher than that for the pristine sample. The AF fluctuations in the doped samples are investigated from a microscopic point of view by the present NMR spectroscopy.

C. ^{13}C NMR spectroscopy

The ^{13}C NMR experiment was performed in a field of 7 T for the pristine sample and 6.7 T for the others. The external magnetic field was applied along the crystalline c direction [Fig. 1(b)], for which the upper critical field is higher than 20 T [10]. Figure 4 shows the NMR spectra of pristine κ-Br,

TABLE I. List of samples.

Sample	^{13}C enriched molecule	T_c (K)	x
pristine	BEDT-TTF	11.2	0%
TTF-7	BEDT-TTF	9.5	7%
TTF-9	BEDT-TTF	9.0	9%
STF-10	BEDT-STF	8.7	10%

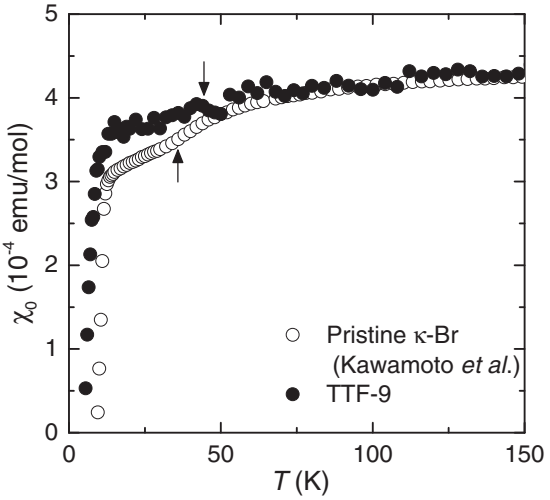

FIG. 3. Temperature dependence of uniform spin susceptibility χ_0 for pristine κ-Br [7] and TTF-9. The core diamagnetism of -4.7×10^{-4} emu/mol is already subtracted. In TTF-9, the deviation from pristine κ-Br was observed below 45 K, as shown by the downward arrow.

TTF-9, and STF-10 obtained at 200 K. The horizontal axis is the NMR frequency shift with respect to the reference material of tetramethylsilan (TMS). For all samples, two distinct peaks

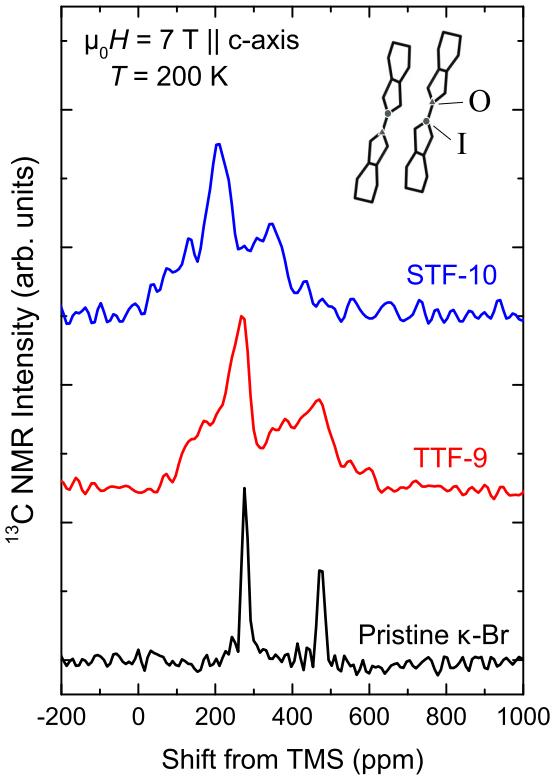

FIG. 4. The ^{13}C NMR spectra of pristine κ-Br, TTF-9, and STF-10 samples at 200 K. Two peaks originating from I and O sites were observed in all samples. The spectral width becomes large in the BEDT-STF dopes samples, but the peak shift was observed only in STF-10.

were observed. In principle, as κ-Br salt possesses eight independent ^{13}C sites in a magnetic field, eight NMR peaks, one from each ^{13}C site, would be expected. When the field is parallel to the c direction, however, every four peaks are superposed, and thus a two-peak structure is observed. These two sites originate from the two nonequivalent carbon sites of the central C=C bonds. Each side of the C=C bond becomes nonequivalent when two BEDT-TTF molecules form a dimer. One site that is close to the center of the BEDT-TTF dimer is called the inner site, and the other is called the outer site, as shown in the inset of Fig. 4. According to the peak assignment reported by Soto *et al.* [11], we assigned the peaks at 277 and 474 ppm to the inner (I) and outer (O) sites, respectively. The spectral width of the TTF-9 sample is much broader than that of pristine κ-Br because of the inhomogeneity introduced by BEDT-STF doping. However, we could not resolve the signal from BEDT-TTF sites close to or far from the BEDT-STF sites in our NMR spectrum.

The nuclear spin-lattice relaxation rate $1/T_1$ was measured using the conventional saturation-recovery method. We integrated the NMR intensity of both I and O sites to obtain the recovery profile of the nuclear magnetization, because at low temperatures the two peaks become broad and merge to form a single peak. As $1/T_1$ for the I site (T_1^{I}) and the O site (T_1^{O}) are different, we used a two-exponential function to fit the recovery profile,

$$\frac{M_0 - M(t)}{M_0} = A\left[0.5\exp\left(-\frac{t}{T_1^{\mathrm{O}}}\right) + 0.5\exp\left(-\frac{t}{T_1^{\mathrm{I}}}\right)\right]. \tag{1}$$

Here, $M(t)$ and M_0 represent nuclear magnetization at t and at thermal equilibrium, respectively, When a well-separated two-peak spectrum is observed at high temperatures, T_1^{I} and T_1^{O} can be measured independently. From the separately obtained T_1^{I} and T_1^{O} at high temperatures in pristine κ-Br, the ratio $T_1^{\mathrm{I}}/T_1^{\mathrm{O}}$ appears to be temperature-independent, and its value is approximately 3.0. This is because ^{13}C nuclear spins at the I and O sites couple to the same π electron spins, and the difference between T_1^{I} and T_1^{O} originates only from the strength of the hyperfine coupling. Therefore, we fixed the ratio $T_1^{\mathrm{I}}/T_1^{\mathrm{O}} = 3$ for the entire temperature range in all the samples. Figure 5 shows the nuclear magnetization recovery profiles for various samples and temperatures. All the profiles fall onto a single curve even in the SC state, when the horizontal axis is scaled by T_1^{I} determined from the fitting. The good scaling by T_1^{I} confirms that the recovery curves always follow the two-exponential function written in Eq. (1), and thus the above fitting procedure is valid to determine the intrinsic relaxation time.

III. RESULTS AND DISCUSSION

A. Local distortion by BEDT-STF impurity

The NMR shift δ is written in terms of the hyperfine coupling constant parallel to the external field direction $A_{\parallel}$, uniform spin susceptibility χ_0, and chemical shift σ as

$$\delta^i = A_{\parallel}^i \rho \chi_0 + \sigma. \tag{2}$$

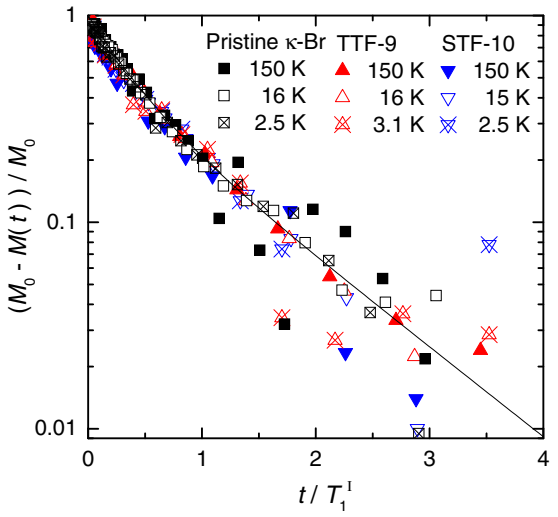

FIG. 5. Relaxation profiles of nuclear magnetization in various samples at various temperatures. The horizontal axis is normalized by T_1^{I} for each condition. All the relaxation profiles follow the same function written in Eq. (1) and shown as a solid line. The good fit to the solid curve confirms the validity of Eq. (1).

Here, i represents the ^{13}C sites I or O. σ is independent of i because both ^{13}C sites are located on the same molecular orbital. In this equation, the hyperfine coupling constant A, which is determined by the highest occupied molecular orbital (HOMO), gives rise to the angle dependence of the NMR shift, and the local density of states (DOS) ρ is responsible for the isotropic effects. We introduced ρ in the equation to discuss the inhomogeneous electronic state. Here, we note that ρ is not proportional to the local carrier density but to the DOS at the Fermi energy. When the electronic system possesses spatial inhomogeneity, the local susceptibility can be written as $\rho\chi_0$, and the NMR shift distributes because of the distribution of ρ. Previously, the distribution of ρ was generated by irradiating an x ray to the sample [12,13]. The x-ray irradiation to the κ-Br salts creates defects in the crystalline lattice, which modulate the local electronic states. After the x-ray irradiation, a metallic conductivity appears at high temperatures [14], and the locally modified inhomogeneous electronic states were observed from the NMR spectroscopy as the NMR spectral broadening. In TTF-9, the linewidth of 110 ppm at 200 K (Fig. 4) is much broader than that of 15 ppm in pristine κ-Br, and it is comparable to that in the x-ray irradiated κ-(BEDT-TTF)$_2$Cu[N(CN)$_2$]Cl (75 ppm at 170 K) [13]. The large distribution of δ in BEDT-STF-doped samples suggests that the BEDT-STF molecules modify the local electronic state. The BEDT-STF doping is more suitable to study impurity effects than the x-ray irradiation to the samples, because we can introduce impurity molecules uniformly in the sample, whereas x-ray damage appears mainly on the surface of a crystal. In addition to this, we can explore the electronic state exactly at the impurity site by a selective enrichment of ^{13}C nuclei to the BEDT-STF molecules.

We revealed the locally distributed electronic state in TTF-9 from the broad NMR spectrum. In contrast to the significant line broadening, the peak positions of TTF-9 are identical to those of pristine κ-Br. This result suggests that the electronic state is modified only near the BEDT-STF molecules, and the doping effect on the uniform susceptibility χ_0 is small as χ_0 is the average over the entire sample. In fact, the impurity effects on χ_0 are small at high temperatures, as shown in Fig. 3.

The NMR spectrum for the impurity site is obtained in STF-10, in which the shift in peak positions is observed in addition to the broadening. The comparable linewidth between STF-10 and TTF-9 strongly suggests that no localized moments are induced at or near the BEDT-STF sites. For STF-10, the peak position can shift because σ, which is not directly related to ρ, is different between BEDT-TTF and BEDT-STF molecules. To study the local electronic state at the impurity site, we investigate the peak separation $\Delta\delta = \delta^{\mathrm{O}} - \delta^{\mathrm{I}} = (A_{\parallel}^{\mathrm{O}} - A_{\parallel}^{\mathrm{I}})\rho\chi_0$, which is independent from σ. We found that $\Delta\delta$ for STF-10 is 1.43 times smaller than that for pristine κ-Br, which indicates that $(A_{\parallel}^{\mathrm{O}} - A_{\parallel}^{\mathrm{I}})\rho$ is reduced by 1.43 at the impurity site. As a molecular orbital calculation by the MOPAC 2012 program indicates that the electronic structure at the ^{13}C site is nearly identical between BEDT-TTF and BEDT-STF molecular orbitals, $A_{\parallel}$ should be almost the same between two molecules. Therefore, we propose a decrease in ρ at the impurity site. In our ^{13}C enriched BEDT-STF molecules, $A_{\parallel}$ is not strongly modified because the ^{13}C site is located at the far side from the Se atoms on the central C=C bond, which is shown as the molecule C in Fig. 1(a).

B. Normal-state magnetic susceptibility

The uniform susceptibility is almost unchanged by BEDT-STF doping at temperatures higher than 50 K, and the small deviation from the pristine sample was observed below 45 K. As the NMR relaxation rate $1/T_1$ is one of the best probes to study the magnetic fluctuations, we measured $1/T_1$ and clearly observed the suppression of the AF fluctuation around 50 K. As shown in Fig. 6, pristine κ-Br shows a maximum of $1/T_1T$ at $T^* = 50$ K, below which $1/T_1T$ decreases and finally shows the temperature-independent Fermi liquid behavior just above

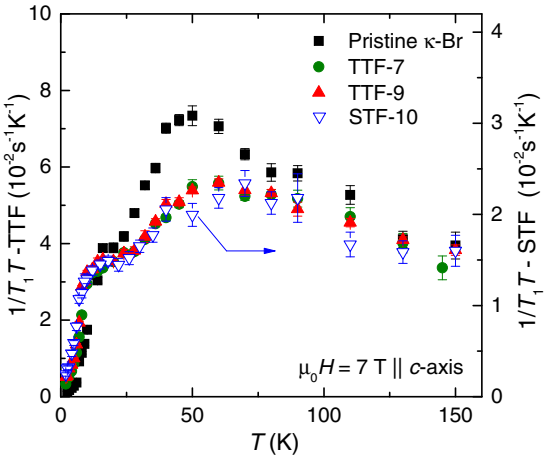

FIG. 6. Temperature dependence of $1/T_1T$ for all samples. The results of pristine κ-Br, TTF-7, and TTF-9 are plotted with the left axis, and the results of STF-10 are plotted with the right axis, which is multiplied by a factor of 2.4. In this scale, TTF-9 and STF-10 show the same temperature dependence.

T_c. In TTF-7 and TTF-9, the peak behavior of $1/T_1T$ around T^* is reduced, and the Fermi liquid behavior was observed from temperatures higher than that in pristine κ-Br.

Generally, $1/T_1$ is written in terms of dynamical susceptibility $\chi''(q)$ as

$$\frac{1}{T_1T} = \frac{2\gamma_n^2 k_B}{\gamma_e^2\hbar^2}\sum_q (\rho A_\perp)^2 \frac{\chi''(q)}{\omega}, \tag{3}$$

where γ_n, γ_e, k_B, and $\hbar$ are the gyromagnetic ratio of the nucleus and electrons, the Boltzmann constant, and the Planck constant, respectively. $A_\perp$ and ω are hyperfine coupling constants perpendicular to the field direction and the NMR frequency. In the case of κ-Br salt, the AF term, which originates from the enhanced susceptibility with the wave vector close to the ordering vector Q, causes the temperature dependence of $1/T_1T$, and $\chi''(q)$ from the long wavelength gives rise to the constant contribution [15]. Therefore, the total $1/T_1T$ can be divided into two terms,

$$\frac{1}{T_1T} = \frac{2\gamma_n^2 k_B}{\gamma_e^2\hbar^2}(\rho A_\perp)^2\left(\sum_{q\simeq Q}\frac{\chi''(q)}{\omega} + \sum_{q\neq Q}\frac{\chi''(q)}{\omega}\right) \tag{4}$$

$$= \left(\frac{1}{T_1T}\right)_{\rm AF} + \left(\frac{1}{T_1T}\right)_{\rm const}. \tag{5}$$

At high temperatures above 100 K, the total $1/T_1T$ values are independent of BEDT-STF concentration, which indicates that the constant term is not affected by the BEDT-STF doping. The AF term increases at low temperature due to the increase in the AF fluctuations. The temperature dependence of the AF term is determined by the dynamical susceptibility at $q = Q$, χ_Q, the AF correlation length ξ, and its energy Γ in the Lorentz-type dynamical susceptibility written as [15]

$$\chi(q,\omega) = \frac{\chi_Q}{1 + (q-Q)^2\xi^2 - i\omega/\Gamma}. \tag{6}$$

The almost same temperature dependence for all samples above 100 K suggests that Γ is not modified by the BEDT-STF doping. At low temperatures, where ξ exceeds the mean impurity-impurity distance l, the AF term is suppressed by the effects of BEDT-STF impurity scattering, which limits ξ to l, and thus the peak near T^* is reduced. The suppression of the AF term near T^* was observed in the x-ray irradiated κ-(BEDT-TTF)$_2$Cu(NCS)$_2$ salt, in which the AF correlation is disturbed by the lattice defects [12]. In contrast, when a mechanical pressure is applied to κ-Br salt, the constant term is reduced because of the increase in bandwidth, and as Γ increases with bandwidth, the AF term is suppressed from high temperatures [16,17]. In the BEDT-STF-doped samples, since the constant term and Γ are independent of the doping concentration, we conclude that the band structure is not modified by the BEDT-STF doping up to 10%.

The bulk effect of the BEDT-STF impurity has been revealed by studying TTF-7 and TTF-9. Next, the local effect at the BEDT-STF site can be investigated by measuring STF-10. The result of $1/T_1T$ measurement on STF-10 is shown in Fig. 6 with the right scale. The temperature dependence of $1/T_1T$ in STF-10 can be scaled to TTF-9 in the entire temperature range by multiplying by a factor of 2.4. The identical temperature dependence between the impurity and bulk sites suggests that the magnetism at both sites has the same origin, confirming our assumption that the local susceptibility is written as $\rho\chi_0$. Therefore, this scaling factor is mainly explained by the small ρ at the BEDT-STF site. From the NMR shift measurement, ρ at the BEDT-STF site was estimated as 1.43 times smaller than that for the BEDT-TTF site. As $1/T_1T$ is proportional to ρ^2, $1.43^2 = 2.04$ is, within our experimental accuracy, in good agreement with the scaling factor of 2.4.

The same temperature dependence at BEDT-TTF and BEDT-STF sites strongly suggests that no strong magnetism has been induced by BEDT-STF doping. This result is consistent with the moderate broadening of NMR spectra at the BEDT-STF sites. In a case of nonmagnetic Zn doping to a YBCO cuprate, a staggered moment is induced near the nonmagnetic impurity. Such a drastic impurity effect is not observed in κ-Br salt, because the substitution of two selenium atoms for sulfur atoms does not strongly modify the overall HOMO structure, which consists of eight sulfur and ten carbon atomic orbitals, and also does not modify the carrier number in the HOMO orbital. We conclude that the BEDT-STF impurity brings about a weak potential disorder in the conduction band.

The impurity potential of BEDT-STF molecules can be estimated by calculating the binding energy of HOMO for BEDT-TTF $E_{\rm TTF}$ and BEDT-STF $E_{\rm STF}$. We calculate the binding energy numerically using MOPAC as $E_{\rm TTF} = -6.98$ eV and $E_{\rm STF} = -6.71$ eV. In κ-Br salt, two BEDT-TTF molecules form a dimer, and the antibonding orbital of the dimer is at the Fermi energy. When we assume that the intradimer transfer energy of a dimer is 0.25 eV [18], the energy for the antibonding orbital of the BEDT-TTF=BEDT-STF dimer can be calculated as -6.56 eV, which is 0.17 eV higher than the energy for the BEDT-TTF dimer. This impurity potential is smaller than the typical bandwidth of 0.6 eV [19], and thus it can scatter weakly the conduction electrons. We can assume that the impurity scattering occurs mainly at the BEDT-TTF=BEDT-STF dimers, as the concentration of a dimer with two BEDT-STF molecules is only 1% when the BEDT-STF doping concentration is 10%,

Here, we comment on the metallic resistivity induced by BEDT-STF doping [5]. From our previous NMR study on x-ray irradiated samples [12,13], we have shown that the resistivity maximum around 100 K is caused by the scattering of conduction electrons brought about by the motion of an ethylene end group, and the coupling between conduction electrons and ethylene motion becomes weak when lattice defects are introduced by x-ray irradiation. We speculate that the BEDT-STF doping also reduces this coupling to induce metallic resistivity.

C. Superconducting pair-breaking effect

In the normal state, the small potential disorder appears to be detrimental to the long-range magnetic correlations near T^*. In this subsection, we discuss the impurity scattering effect on superconducting properties. For pristine κ-Br in 7 T, $1/T_1$ shows a power-law temperature dependence proportional to T^3 below T_c. Then at very low temperatures, the temperature dependence becomes weak since the external magnetic field populates the quasiparticle excitations near the nodes on the SC gap. This behavior is characteristic of unconventional

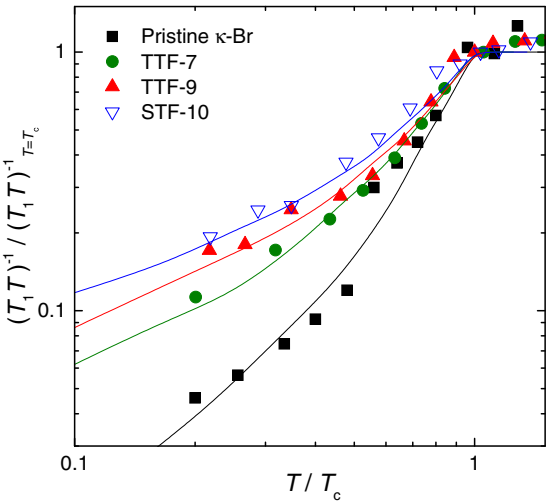

FIG. 7. Temperature dependence of $1/T_1T$ in the SC state. The horizontal axis is the reduced temperature T/T_c. For the vertical axis, $1/T_1T$ is normalized by the value of $1/T_1T$ at T_c. Solid lines are the results of our model calculation.

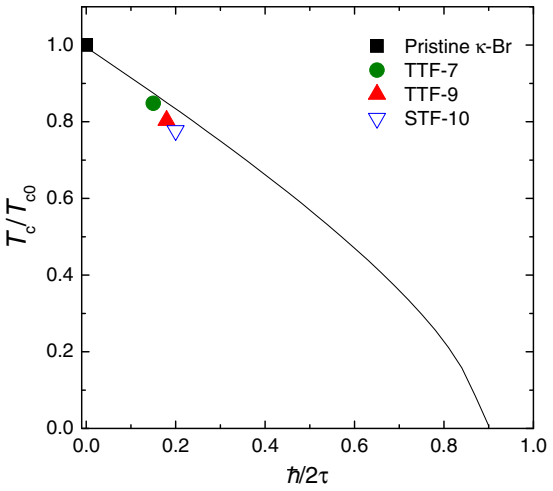

FIG. 8. Reduction of T_c as a function of impurity scattering rate $\hbar/2\tau$. The solid curve represents the AG relation [Eq. (8)]. T_c of BEDT-STF doped samples are consistently explained by the SC pair breaking effect of impurity scattering.

superconductivity. We simulate the temperature dependence of $1/T_1T$ in the SC state using a model for d-wave superconductivity. The experimental results are consistently explained by our calculation, as shown in Fig. 7.

In TTF-7 and TTF-9, $1/T_1T$ at the lowest temperature increases with doping concentration. As $1/T_1T$ at the lowest temperature is determined by the quasiparticle DOS, the increase in $1/T_1T$ by doping indicates that the impurity scattering populates additional excitations. This result reveals qualitatively that the doped BEDT-STF molecules scatter SC Cooper pairs and suppress superconductivity.

To quantitatively investigate the impurity scattering effect, we estimate the impurity scattering rate $\hbar/2\tau$ by fitting the temperature dependence of $1/T_1T$ to our model. We can calculate the quasiparticle DOS modulated by impurity scattering using the Green's function derived from the Eilenberger equation [20].

$$g = \frac{\omega_l + \hbar\langle g\rangle/2\tau}{\sqrt{(\omega_l + \hbar\langle g\rangle/2\tau)^2 + |\Delta|^2|\phi|^2}}. \qquad (7)$$

Here, ω_l is the Matsubara frequency, while Δ and ϕ are the gap function and anisotropy factor, respectively. In the case of a two-dimensional d-wave superconductor, $\phi = \cos 2\theta$. The temperature dependence of $1/T_1T$ is calculated from this quasiparticle DOS. The results for TTF-7, TTF-9, and pristine κ-Br are shown in Fig. 7 as solid lines. Even for pristine κ-Br, a good fit is obtained with finite $\hbar/2\tau$. We assume that the scattering in pristine κ-Br is caused by the vortex cores. Even though the vortex contribution should be the same for all samples measured in comparable magnetic fields, $\hbar/2\tau$ increases systematically with BEDT-STF doping. We therefore state that for TTF-7 and TTF-9, the increase in $\hbar/2\tau$ is caused by impurity scattering. The impurity contribution of $\hbar/2\tau$ is 0.15 and 0.18 for TTF-7 and TTF-9, respectively, and $\hbar/2\tau = 0.20$ for STF-10. A more sophisticated calculation, which involves the quasiparticle excitations by Doppler shift, will be required to compare the results obtained in different magnetic fields.

As we have estimated the scattering rate for each sample, we can in principle calculate T_c of each sample from the Abrikosov-Gorkov (AG) equation [21],

$$\ln\frac{T_c}{T_{c0}} + 2\pi k_B T_c \sum_{l=0}^{\infty}\left(\frac{1}{\omega_l} - \frac{1}{\omega_l + \hbar/2\tau}\right) = 0. \qquad (8)$$

In Fig. 8, T_c of each sample is plotted as a function of $\hbar/2\tau$, together with the theoretical curve calculated from Eq. (8). Here, $T_{c0} = 11.2$ K is the SC transition temperature of our pristine κ-Br. The good fit to the theoretical curve suggests that in the BEDT-STF-doped samples, T_c is reduced mainly by the impurity scattering effect. This is the first microscopic evidence to demonstrate the impurity scattering effects in organic superconductors. We note that the observed T_c appears slightly lower than the solid curve for all samples. This result might suggest that T_c is suppressed by an additional effect other than the impurity scattering, such as the suppression of AF fluctuations.

In STF-10, the local effects of quasiparticle scattering would be observed. At a doping concentration of 10%, however, $1/T_1T$ at the impurity sites shows the same temperature dependence as that at the bulk sites. Similar to the high-temperature magnetic susceptibility, superconducting properties are also uniformly affected by impurities. The in-plane SC coherence length in κ-Br has been measured as approximately 30 Å [22,23], whereas the mean distance between BEDT-STF impurities at 10% is estimated as $l = 17$ Å from the in-plane lattice constants $a = 12.942$ Å and $c = 8.539$ Å [24] [Fig. 1(b)]. These length scales indicate that ten BEDT-STF molecules are located within the coherence volume. Therefore, a Cooper pair is scattered by several impurities within the coherence time, which results in a uniform quasiparticle state even at the impurity site. An experiment at a smaller doping concentration, in which one impurity exists in a coherence

volume, is required to investigate the scattering effect from a single impurity.

IV. SUMMARY

We performed ^{13}C NMR measurements in pristine and BEDT-STF-doped κ-Br. In the normal state, we observed that the peak behavior of $1/T_1T$ at 50 K becomes small after doping, while the constant term remains unchanged. From this behavior, we suggest that the BEDT-STF doping does not modify significantly the band structure, but it limits the antiferromagnetic correlation length by impurity scattering. In the superconducting state, we observed the recovery of $1/T_1T$ at the lowest temperature in the doped samples, which addresses the quasiparticle excitations by the potential scattering at the BEDT-STF sites. We conclude that the reduction of T_c in BEDT-STF-doped samples originates mainly from the SC pair breaking effect of impurity scattering. We estimated the scattering rate from the temperature dependence of $1/T_1T$ in the SC state. The results were consistently explained by the AG theory. A slight deviation from the theoretical curve might suggest that the suppression of magnetic fluctuations also reduces T_c. By measuring the ^{13}C NMR signal in STF-10, we observed the electronic state exactly at the impurity sites. Although $1/T_1T$ is smaller by a factor of 2.4 than that at the BEDT-TTF sites, the temperature dependence is identical both in the normal and SC states. At the doping concentration of approximately 10%, many BEDT-STF impurities exist within the antiferromagnetic correlation length and the SC coherence length. Therefore, the impurity scattering effect is averaged even at the impurity sites. The present results revealed microscopically the BEDT-STF doping effects on BEDT-TTF-based organic salts. As diverse physical properties have been observed in the BEDT-TTF-based organic salts, the effects of potential disorder on various ground states can be investigated using this BEDT-STF doping technique.

ACKNOWLEDGMENTS

We would like to acknowledge K. Kita and C. J. Gómez-García for useful discussions. T.K. is financially supported by the Ushio Foundation. This work is partially supported by Japan Society for the Promotion of Science KAKENHI Grant No. 25610082.

[1] A. Balatsky, I. Vekhter, and J.-X. Zhu, Rev. Mod. Phys. **78**, 373 (2006).
[2] T. Masui, N. Suemitsu, Y. Mikasa, S. Lee, and S. Tajima, J. Phys. Soc. Jpn. **77**, 074720 (2008).
[3] Y. Kitaoka, K. Ishida, and K. Asayama, J. Phys. Soc. Jpn. **63**, 2052 (1994).
[4] H. Alloul, J. Bobroff, M. Gabay, and P. J. Hirschfeld, Rev. Mod. Phys. **81**, 45 (2009).
[5] T. Naito, A. Miyamoto, H. Kobayashi, R. Kato, and A. Kobayashi, Chem. Lett. **21**, 119 (1992).
[6] G. E. Pake, J. Chem. Phys. **16**, 327 (1948).
[7] A. Kawamoto, K. Miyagawa, Y. Nakazawa, and K. Kanoda, Phys. Rev. B **52**, 15522 (1995).
[8] A. Kawamoto, K. Miyagawa, Y. Nakazawa, and K. Kanoda, Phys. Rev. Lett. **74**, 3455 (1995).
[9] T. Sasaki, N. Yoneyama, A. Matsuyama, and N. Kobayashi, Phys. Rev. B **65**, 060505 (2002).
[10] G. Saito, H. Yamochi, T. Nakamura, T. Komatsu, T. Ishiguro, Y. Nogami, Y. Ito, H. Mori, K. Oshima, M. Nakashima, S. Uchida, H. Takagi, S. Kagoshima, and T. Osada, Synth. Met. **42**, 1993 (1991).
[11] S. M. De Soto, C. P. Slichter, A. M. Kini, H. H. Wang, U. Geiser, and J. M. Williams, Phys. Rev. B **52**, 10364 (1995).
[12] M. Matsumoto, H. Kato, Y. Kuwata, A. Kawamoto, N. Matsunaga, and K. Nomura, J. Phys. Soc. Jpn. **81**, 114709 (2012).
[13] M. Matsumoto, Y. Saito, and A. Kawamoto, Phys. Rev. B **90**, 115126 (2014).
[14] K. Sano, T. Sasaki, N. Yoneyama, and N. Kobayashi, Phys. Rev. Lett. **104**, 217003 (2010).
[15] E. Yusuf, B. J. Powell, and R. H. McKenzie, Phys. Rev. B **75**, 214515 (2007).
[16] H. Mayaffre, P. Wzietek, C. Lenoir, D. Jérome, and P. Batail, Europhys. Lett. **28**, 205 (1994).
[17] M. Itaya, Y. Eto, A. Kawamoto, and H. Taniguchi, Phys. Rev. Lett. **102**, 227003 (2009).
[18] K. Oshima, T. Mori, H. Inokuchi, H. Urayama, H. Yamochi, and G. Saito, Phys. Rev. B **38**, 938 (1988).
[19] K. Kanoda, Hyperfine Interact. **104**, 235 (1997).
[20] N. B. Kopnin, *Theory of Nonequilibrium Superconductivity*, The International Series of Monographs on Physics, Oxford Science Publications (Clarendon, New York, 2001).
[21] A. A. Abrikosov and L. P. Gor'kov, Sov. Phys. JETP **12**, 1243 (1961).
[22] M. Lang, F. Steglich, N. Toyota, and T. Sasaki, Phys. Rev. B **49**, 15227 (1994).
[23] M. Dressel, O. Klein, G. Grüner, K. D. Carlson, H. H. Wang, and J. M. Williams, Phys. Rev. B **50**, 13603 (1994).
[24] A. M. Kini, U. Geiser, H. H. Wang, K. D. Carlson, J. M. Williams, W. K. Kwok, K. G. Vandervoort, J. E. Thompson, and D. L. Stupka, Inorg. Chem. **29**, 2555 (1990).